AD-A191 887 INFRARED DEVICES USING SEMICONDUCTOR QUANTUM WELLS(U) 1/1
ROYAL SIGNALS AND RADAR ESTABLISHMENT MALVERN (ENGLAND)
M J KANE ET AL. OCT 87 RSRE-MEMO-4018 DRIC-BR-104732

UNCLASSIFIED F/G 9/1 NL

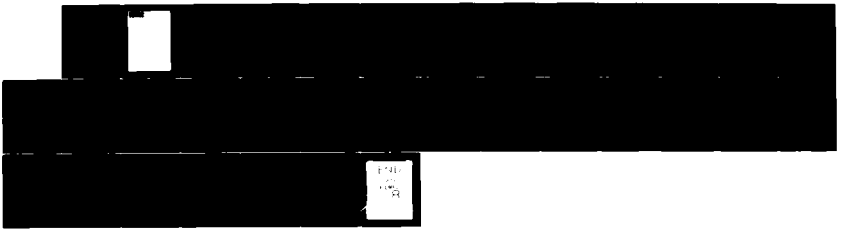

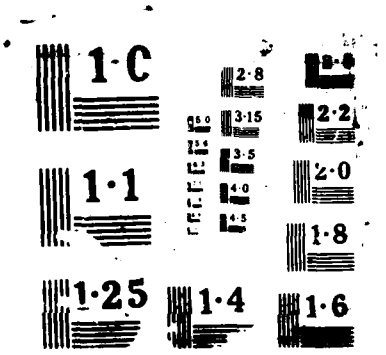
1·C
1·1
1·25
1·4
2·8
3·15
3·5
4·0
4·5
2·2
2·0
1·8
1·6

RSRE MEMORANDUM No 4018

# INFRARED DEVICES USING SEMICONDUCTOR QUANTUM WELLS

M J KANE AND N APSLEY

## ABSTRACT

We describe in this memo the results of a preliminary calculation which shows how the intersubband optical transition in III-V quantum wells may be used as the basis for research into a family of infrared devices. In particular, we show that resonating the transition with a surface plasmon or with a guided mode in a semiconductor-quantum well- metal structure can enhance its optical effects by roughly a factor of 50. This allows only $4x10^{12}$ carriers per sq. cm to effect total absorption of the incoming radiation. Such a density can be controlled electrostatically and so the transition may be switched by applying a bias to the (Shottky) metal; thus we have an efficient electronic modulator for the 10 micron band. Intersubband absorption should, in addition, show significant photoconductivity and so the device might prove a reasonable infrared detector. Finally, an important consideration of this device is that it is built epitaxially using wide band gap semiconductors. The possibilities, therefore, of substantial monolithic integration are considerable and we allow ourselves some speculation on the types of device which may be possible.

## 1 INTRODUCTION

Semiconductor optical devices for the 10 micron wavelength band are usually made from materials with bandgaps in the same range ($E_g$ ~100 meV), the so called narrow gap semiconductors. Highly successful radiation detectors are made from CdHgTe and InSb and semiconductor lasers based on lead salts are commercially available. Non semiconductors are also useful in this wavelength range. Detectors can be made from pyroelectric substances such as triglycine sulphate. Gas lasers (especially $CO_2$ lasers) work well at these wavelengths. Modulators for these lasers are either non solid state (Pockels or Kerr cells) or are constructed using electrorefractive solids such as some niobates or tantalates.

All of the devices mentioned above are highly developed and successful so that any competing technology must offer substantial advantages. However, the existing devices are all based on rather exclusive technologies suitable for the infrared application only. The purpose of this memorandum is to outline a method whereby quantum well devices fabricated from wider bandgap materials (such as GaAs/AlGaAs) can be made to respond to radiation at 10 microns wavelength and hence provide conventional semiconductors with an infrared capability. It is then possible to propose integration of the infrared device (e.g. a detector) with amplifiers or optoelectronic devices working at other wavelengths.

When electrons are confined in a semiconductor quantum well by a suitable cladding material, a series of quantised energy levels results, whose energy spacing corresponds to radiation in the mid to far infrared (with $\lambda$=~10-30 $\mu$m). (See figures 1 and 2.) Electromagnetic dipole transitions between different subbands are allowed and can have large oscillator strengths. The intersubband transition energy can be tuned (say to a $CO_2$ laser wavelength) by choosing the appropriate well width. This transition forms the basis of the potential electro-optic devices (such as detectors and modulators) described in this memo. In addition to the resonant bound to bound transitions it is also possible for

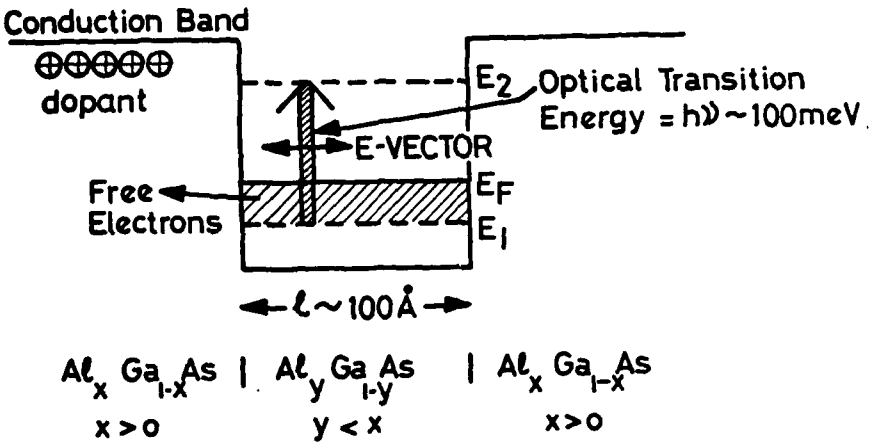


Figure 1 An energy band diagram of the conduction band in a typical quantum well, showing the quantised subbands and the intersubband transition.

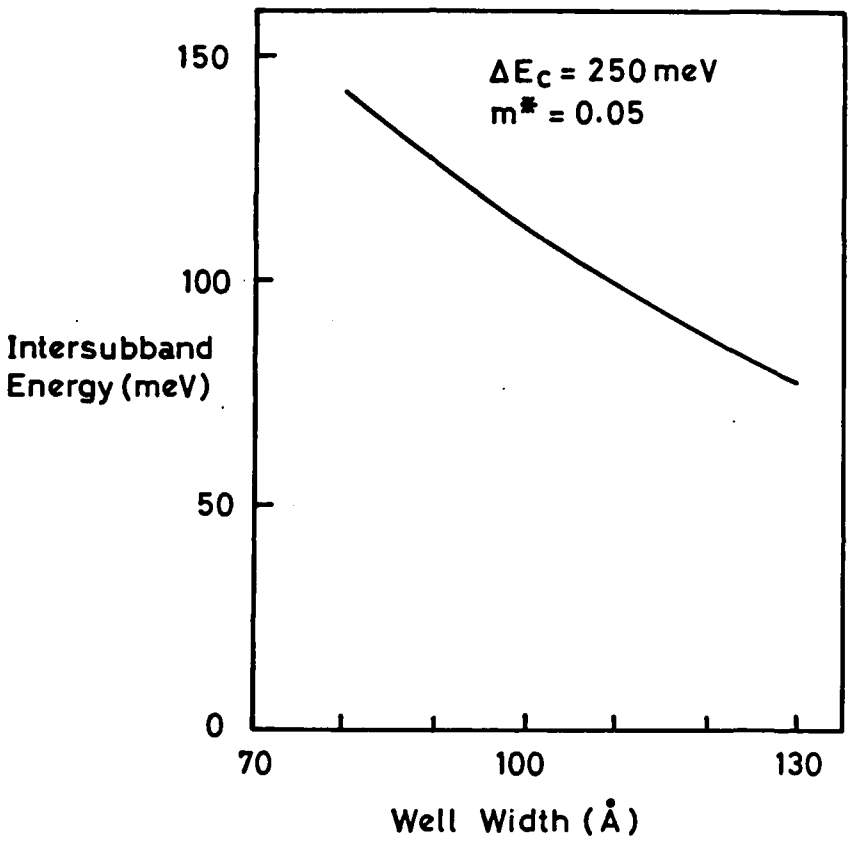


Figure 2 The intersubband spacing for a well of finite (250 meV) depth and an effective mass of 0.05 in both well and barrier. These material parameters are typical of the InP/InGaAs material system. The calculation given here does not include any non parabolicity which tends to make the higher energy states heavier and reduce the intersubband separation.

bound to free transitions (from the bound quantum well states to the continuum of states above the top of the well) to occur. Devices based on these transitions would have a broad band response as opposed to the narrow band resonant devices based on bound to bound transitions.

This memorandum describes theoretical calculations of the optical properties of quantum well devices and test structures involving intersubband transitions. Mathematical details of the calculational methods are given in the appendices while the main body of the memo will concentrate on the results of the calculations. Section 2 will describe how to calculate the properties of modulation doped multiple quantum well test structures, so that the oscillator strengths, linewidths and frequencies of the intersubband transition can be established. Section 3 describes the modelling of an electro-optic modulator based on a novel method of coupling electromagnetic radiation to the intersubband transitions. Appendix 1 describes the dielectric functions used to model the intersubband transition. Appendix 2 describes a method for calculating the optical properties of a multilayer system with anisotropic component layers.

## 2 CALCULATIONS OF THE OPTICAL PROPERTIES OF MULTI QUANTUM WELL SYSTEMS INVOLVING INTERSUBBAND TRANSITIONS

Intersubband transitions are transitions between two states derived from the conduction band so that doped structures must be used in order to have free electrons in the quantum wells. The intersubband transition has a large oscillator strength but is only induced by electric fields oscillating perpendicular to the plane of the quantum well (See appendix 1) Unfortunately, the high refractive indices of semiconductors such as GaAs or InP (typically ~3) tend to refract light incident from air or vacuum so that its electric field lies in the plane of the well and makes the intersubband absorption weak. Nevertheless, quantum well intersubband transitions have been observed directly by several authors[1-3]. Direct observation of the intersubband transitions represents the simplest way of verifying the theory presented in appendix 1 for their energies, strengths and linewidths. (References 1 and 2 report work on modulation doped structures whereas reference 3 describes the properties of anti-modulation doped structures. No significant differences were seen in the optical properties.)

A typical experimental arrangement and results are shown in figure 3a. Multiquantum well structures with 50 wells, each containing $5\text{-}10\text{x}10^{11}$ $cm^{-2}$ carriers are used. The light is P polarised and incident at the Brewster angle. At this angle of incidence there is coupling to the intersubband transitions but no reflection at any of the semiconductor air interfaces and therefore no problem with Fabry-Perot etalon fringes masking real absorption features. The intersubband absorption typically has a peak value of 3-5% and the absorption spectra seen in such circumstances can be calculated using the model outlined in appendices 1 and 2. By fitting the calculated spectra to the observed spectra, values of the parameters used to describe the oscillator strength and linewidths of the intersubband transition in appendix 1 can be determined. The weakness of the absorption in this configuration is due to the inefficiency of coupling to the intersubband transitions rather than to the weakness of the transitions. When MQW structures are used

in a waveguide mode, (see for example references 3 and 4 and figure 3b) very strong intersubband absorption can be obtained.

In our subsequent work we will use transition parameters determined from the absorption spectra of West and Eglash[1] as the basis for calculating the properties of more complicated structures. Typically, an 82 Å wide GaAs well clad by $Al_xGa_{1-x}As$ with x=0.3 has a plasma shifted intersubband absorption peak at 120 meV. The oscillator strength is 0.82 and the linewidth (FWHM) is 20 meV. (This corresponds to a linewidth parameter of $8x10^{12}$ $s^{-1}$ in equation (A1.8). The transition parameters derived from the measurements of other authors (see references 2 and 3) are similar to these.)

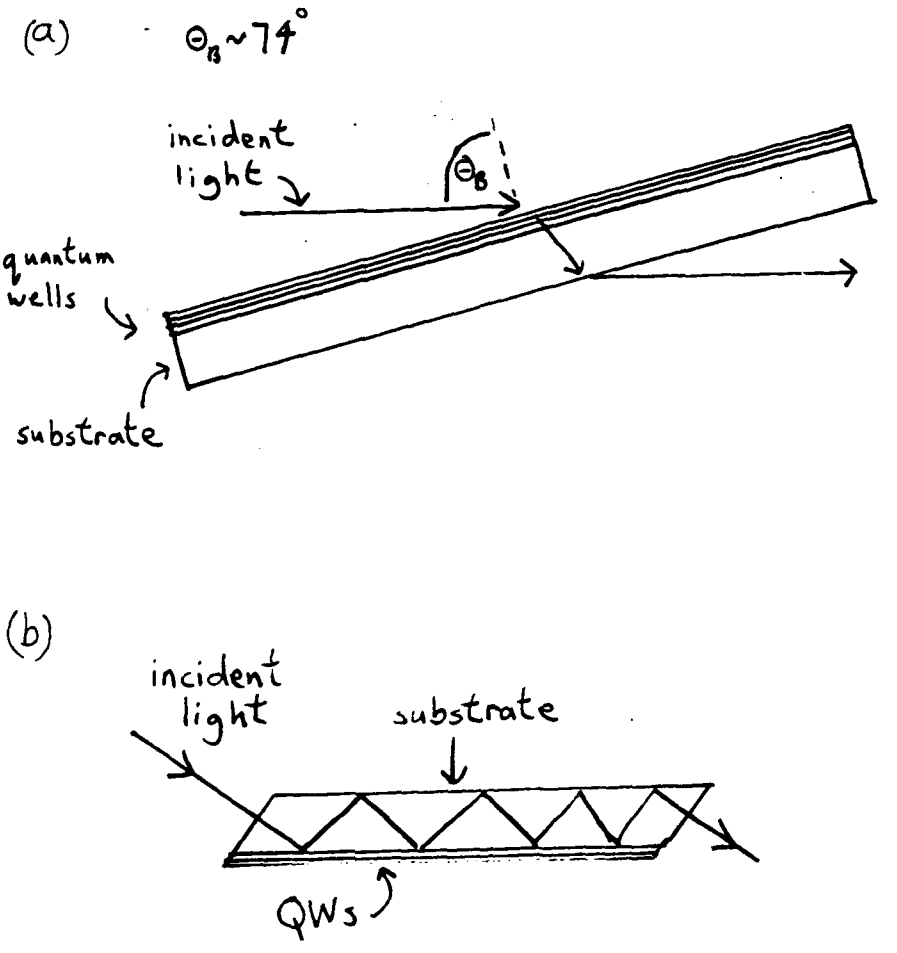


Figure 3 (a) A typical arrangement for measuring the absorption at the Brewster angle. The shallow angle of incidence means that a large area of the sample is sampled.
(b) The waveguide geometry used by Levine et al to see a very strong intersubband absorption.

## 3 QUANTUM WELL DEVICES USING INTERSUBBAND TRANSITIONS

The key feature of any electro-optic device based on intersubband transitions must be an efficient method of coupling radiation to the electronic transition. In this memo we propose a device configuration which gives strong coupling to intersubband transitions. We initially propose to use the device as a reflective modulator at 10 microns wavelengths. However, it may may also be possible to use the device as detector.[4] [5] This would require the electrical properties of the device to be modified in some manner by the intersubband absorption. This may be possible by some photothermal or field assisted tunneling process whereby carriers photoexcited into higher subbands may be able to escape from the quantum well or it may be possible to measure changes in the in-plane resistance of the quantum well because of the lower mobility of the electrons in the higher subband (See for example reference 6.) These processes are not well understood and we will not speculate further on this application.

The structure of the device is shown in figure 4. Essentially, the device consists of a gallium arsenide substrate (dielectric constant 10.9 in this frequency range), a layer of aluminium arsenide (dielectric constant 8.16), ~4 quantum wells (modulation doped) and a metallic overlayer. The device is mounted on a gallium arsenide prism (with surface anti-reflection coatings) in order to couple to incident light. The optical properties of the device are modified by applying a bias to the metal electrode and altering the carrier density in the quantum wells. The number of quantum wells is chosen to be one or two fewer than the maximum number of wells that can be filled or emptied without reaching the breakdown field of the GaAs(AlAs). Maximising the number of wells maximises the changes that can be made to the optical properties by filling or emptying the wells with carriers. The frequency of the intersubband absorption is tuned to the frequency of operation by choosing an appropriate well width. The device can only work with p polarized light.

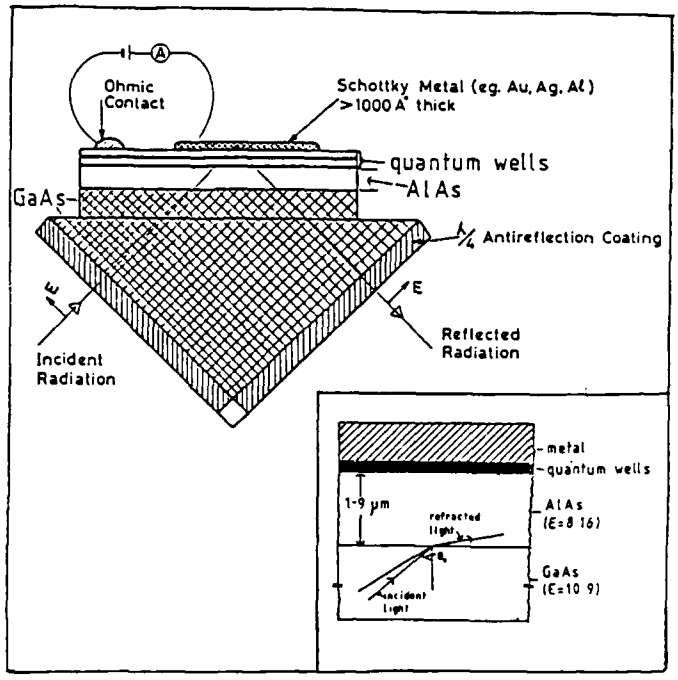


Figure 4 The details of the device structure discussed in this paper, including an expansion of the part containing the quantum wells (the inset).

The optical properties of the device are calculated using the matrix method given in appendix 2. The metal is treated as a electron plasma with an isotropic dielectric function described by equation (A1.14) with $\omega_p$=1.36x10$^{16}$ s$^{-1}$ and $\tau$=2x10$^{-14}$ s The quantum wells are treated as slabs of anisotropic dielectric with dielectric constants as given by equations (A1.9) and (A1.14) the linewidth parameter used is that determined in section 2 from the measurements discussed in the literature.

There are two mechanisms by which this device can work. The first involves launching a surface plasmon along the metal semiconductor interface. The second mode of operation involves launching a guided wave in the AlAs. The surface plasmon is excited when light is incident at an appropriate angle (somewhat greater than the critical angle for total internal reflection at the AlAs/GaAs interface). The electric field in the surface plasmon has a magnitude substantially greater than that of the incident wave and a significant component oscillating perpendicular to the plane of the quantum well. The surface plasmon couples to the intersubband absorption of the quantum wells. When there are carriers in the quantum well the intersubband absorption is sufficiently strong to destroy the surface plasmon. The operation of the device (shown as a plot of reflectivity against angle with and without carriers present) is shown in figure 5. These plots were obtained using the methods described in apendices 1 and 2. The surface plasmon is excited by light incident at 59.9 degrees to the normal. When there are no carriers in the quantum well the excitation of the surface plasmon is seen as a decrease in reflectivity at this particular angle. When there are carriers in the well the intersubband absorption destroys the surface plasmon and nearly all of the light is reflected. In this mode of operation the intersubband absorption is used to control the surface plasmon. Little light is ever absorbed by the quantum wells. The damping of the surface plasmon is a resonant phenomenon. If the intersubband resonance is shifted away from the plasmon frequency then the plasmon absorption dip reappears. The absorption of the energy occurs in the metal when the surface plasmon is excited.

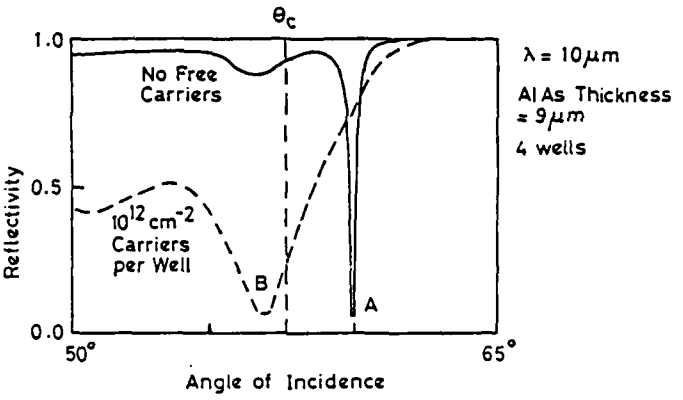


Figure 5 The calculated operation of the device as a modulator shown as plots of reflectivity versus angle both ,with and without carriers present. The operating frequency corresponds to 10 $\mu$m wavelength in free space and the intersubband absorption is tuned to this frequency. This device has a thick 9$\mu$m AlAs layer and contains four quantum wells.

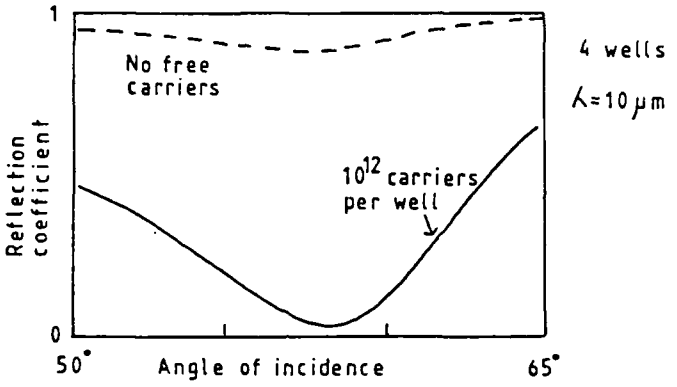


Figure 6 The calculated operation of a device with a thin (2.1 $\mu$m) AlAs layer and four quantum wells. The waveguide mode is stronger and broader than in figure 5

The second mode of operation occurs when light is incident at angles less than the critical angle for total internal reflection at the AlAs/GaAs interface. The light ray is refracted so that it runs almost parallel to the AlAs/GaAs interface and therefore has a large component of its electric field perpendicular to the quantum well. The metal overlayer ensures that the electric field is perpendicular to the plane of the quantum well because it cannot support an electric field in the plane of the quantum well. This light can excite intersubband transitions and be absorbed in the quantum wells. This mode of operation differs from the previous one in that minimum reflection occurs when carriers are present in the quantum well and that the absorption of the energy occurs in the quantum well rather than in the metal. This mode of operation is effective over a much wider angular range than the mode of operation involving surface plasmons. The waveguide mode of operation is most effective when the angle of incidence is such that a standing wave is set up in the AlAs with an antinode at the metal semiconductor interface. For a 9 micron thick layer of AlAs this occurs when the angle of incidence is 57.7. The waveguide mode of operation becomes less sensitive to angle of incidence if the AlAs is thinned down. The optimum thickness of AlAs (i. e. that which gives the greatest absorption) apears to be ~2.1 microns. See figure 6. The reflectivity of this structure can be changed from <5% to >95% by depopulating the quantum wells. The angular range of when such a structure is used as a modulator is >20° for a 50% decrease in modulation efficiency. In the non-reflecting mode all of the incident power is absorbed in the quantum wells.

The distribution of the perpendicular electric field for a device with a 9 $\mu$m AlAs is shown in figure 7. Figure 7a shows the field distribution when the angle of incidence is less than the critical angle for total internal reflection. A standing wave pattern containing one and a half periods is clearly seen. Figure 7b shows the field distribution when when the surface plasmon is excited. The enhancement of $E_z$ is clearly seen. Figure 8 shows the field distribution in a structure with an AlAs thickness of 2.1 $\mu$m. A standing wave

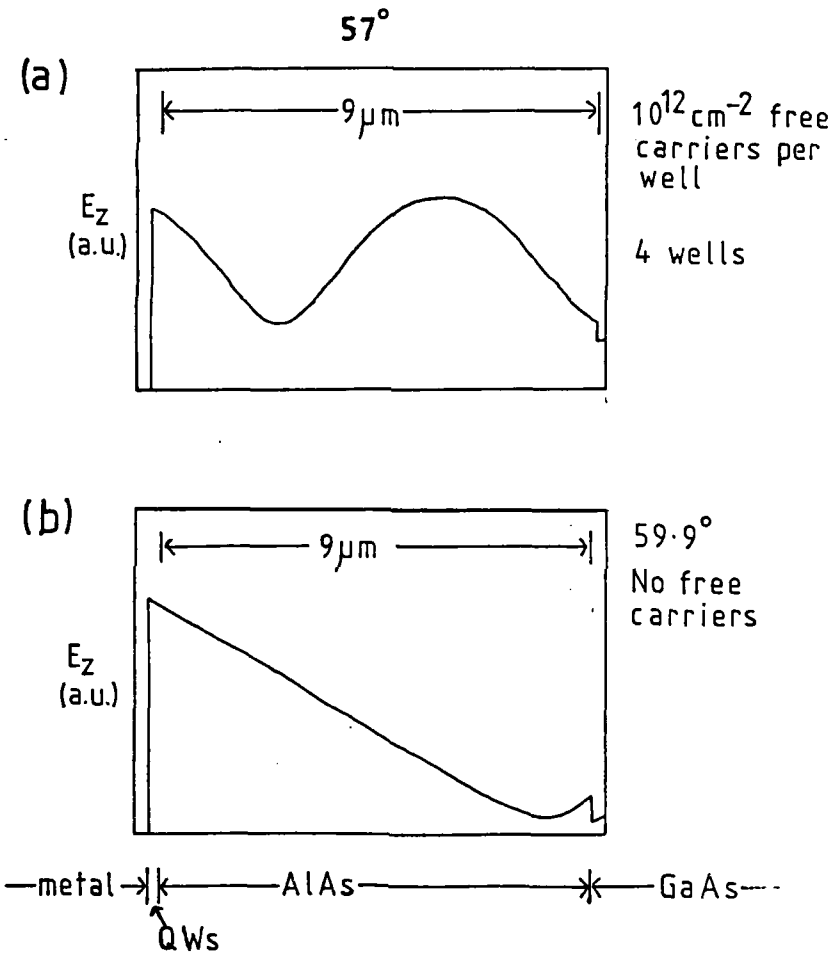


**Figure 7** The calculated internal distribution of the perpendicular electric field $E_z$ for the device structure whose performance is shown in figure 2, for (a) 57° angle of incidence and $10^{12}$ cm$^{-2}$ carriers in each quantum well (waveguide mode) and (b) 59.9° angle of incidence and no free carriers in the quantum wells (surface plasmon mode).

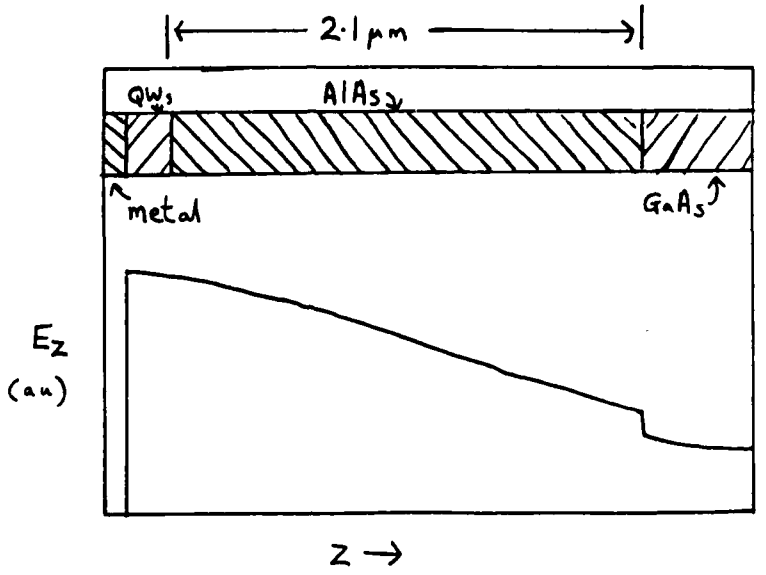


57°

4 wells

$10^{12}$ $cm^{-2}$ carriers per well.

Figure 8 The calculated internal distribution of the perpendicular electric field $E_z$ for the device (with a 2.1 μm AlAs layer) whose operation is shown in figure 6 for an angle of incidence of 57° and $10^{12}$ $cm^{-2}$ carriers $cm^{-2}$

is again obtained because the angle of incidence is less than the critical angle. Approximately half a period of a standing wave is seen in the AlAs.

## 4 CONCLUSIONS

In memo we have shown how the optical cross-section of the quantum well intersubband transition can be increased to produce large scale effects. Straightforward applications are obvious. The device may be used as a modulator for narrow band sources (eg carbon dioxide lasers) in the 10 micron band.

A narrow band photoconductive detector using semiconductor quantum wells has recently been demonstrated by Levine et al[4]. A bias is applied across the quantum well which enables electrons in the excited state to tunnel out of the well and thus photoconduct. In its simplest form this detector will not address the temperature problem. The two states are as thermally connected as they are optically and so the device will require cooling. It should be noted, however, that the guided wave methods of optical enhancement proposed here do lend themselves to separating the two effects. If the "guides" are terminated laterally, then the radiation may be trapped and so only a small proportion of the total optical crossection need contain quantum wells, the only significant absorption mechanism present. In this manner optical and thermal crossections may be made different but quantitative evaluation of this effect awaits further experiments.

Throughout the discussion, we have used a geometric, attenuated total internal reflection coupling scheme. Experimental investigations will no doubt be conducted this way and the system, as has been shown, is readily described theoretically. Alternative coupling schemes, based on surface corrugation or gratings, are equally good at exciting these modes, once correctly designed and optimised. A "real" device would almost certainly employ such a method, the main advantage being that angular acceptance of the device would be more readily matched to the f-number of an optical system.

Of primary importance with respect to this device, is that it is constructed of wide band gap semiconductors on a wide band gap substrate. This means that integration with

FET amplifiers or logic control circuits is a very real possibility, the many technological problems notwithstanding. More exciting, we believe is the propect of integration with optoelectronic devices working at shorter wavelengths. Suppose, for instance this device, working in photoconductive mode, were grown in series with an interband quantum well, spatial light modulator tuned for the visible red. Such a device then, correctly pixelated etc. of course, would allow a thermal scene to be imaged in the visible, without the need for any intervening electronics. Equally, the process could be reversed if optical processing using infrared lasers becomes dominant.

Our conclusion then is that we have shown how, at least in principle, quantum wells in wide band gap III-V alloys can be given a significant reponse in the medium infrared, and so offer a range of device possibilities, hitherto unequalled in any single materials system. Only further experimental investigations will reveal to what extent nature matches our expectations.

ACKNOWLEDGEMENTS

We would like to thank Colin Brewitt-Taylor for showing us how to perform the anisotropic multilayer matrix calculations.

## APPENDIX 1: SUBBAND ENERGIES AND TRANSITION STRENGTHS

The presence of a quantum well in the xy plane in a semiconductor results in the quantisation of electron motion in the z direction but allows free motion in the x y plane. The energies of an electron in the quantum well are given by the expression

$$E_i(k) + \frac{\hbar^2 k^2}{2m_i^*} \qquad \text{(A1.1)}$$

where k is the wavevector for motion in the x y plane. (The $E_i$ are only weak functions of k for typical energies encounterd in quantum wells.) The $E_i$s can, to a first approximation be evaluated by solving the Schrodinger equation for a finite square potential well in a very similar manner to that described in all quantum mechanics text books. The effective mass of the electron is different in the quantum well and cladding and is also energy depenedent due to the non parabolic nature of the conduction bands. The mass difference in the well and cladding is taken into account by using current conserving boundary conditions. The nonparabolicity is treated by making the effective mass energy dependent according to the relation

$$\frac{1}{m^*} = \frac{1}{m_0}\left(1 + \frac{2K_2 E}{E_g}\right) \qquad \text{(A1.2)}$$

where $m^*$ is the effective mass

$m_0$ is the band edge effective mass

$K_2$ is the non parabolicity constant (−0.95 for InGaAs and −1.4 for GaAs)

$E_g$ is the band gap of the semiconductor.

Figure 6 shows the subband energies as a function of well width for the InGaAs system. As the well narrows the number of bound states decreases. The bound states change continuously into unbound states as the electron wavefunction penetrates deeper into the cladding. The weak coupling of the motion of the electrons in the x y plane to that in the z direction means that it is possible for bound states with large values of $k_x$

or $k_y$ to exist at energies above the top of the well.

The presence of a significant electron density in the quantum well bends the conduction bands over with a negative curvature alters the position of the subbands. The shift of the energy levels can be treated adequately using first order perturbation theory for wells of widths of interest to us here (~100 Å) and typically reduces the subband spacing by ~2meV in ~100 meV.

The $E_i$ are functions of k because the boundary conditions at the well cladding interface requires that the in plane component of the wavevector be conserved so that the kinetics energy of the transverse motion is different in the well and cladding. This reduces the effective height by an amount

$$\left(1 - \frac{m_{well}}{m_{clad}}\right) E$$

This results in a lower subband spacing for electrons at the Fermi energy than for electrons at k=0 and makes a significant contribution to the linewidth (see later).

We will now consider the properties of the transition between the lowest and first excited subbands. The wavefunctions of these two states can be written in the form

$$\psi_0 = F_0(z)u_0(r) \qquad \text{(A1.3)}$$

$$\psi_1 = F_1(z)u_0(r) \qquad \text{(A1.4)}$$

where $u_0(r)$ is the Bloch function of the conduction band and $F_0(z)$ and $F_1(z)$ are the envelope functions of the subband. $F_0(z)$ has even parity and $F_1(z)$ has odd parity. Dipole transitions between these two states will only be caused by an electric field oscillating in the z direction i.e. perpendicular to the plane of the quantum well. The quantum mechanical transition operator can be written as

$$eE_z z e^{i\omega t} \qquad \text{(A1.5)}$$

Intersubband transitions are transitions between two states derived from the conduction band. Structures must be doped in order to observe such transitions.

Now using the standard quantum mechanical approach to the absorption of radiation (see for example Dicke and Wittke, An Introduction to Quantum Mechanics pp272–277), the rate of energy absorption W is given by

$$W = \frac{N_{3d} e^2 E_z^2}{2\hbar^2 \omega^2} |\langle f|z|i\rangle|^2 \omega_{fi}^2 \hbar\omega \frac{\Gamma}{\Gamma^2 + (\omega_{fi}-\omega)^2} \qquad \text{(A1.6)}$$

where $N_{3d}=N_{2d}/a$ and is the bulk carrier density, $|f\rangle$ and $|i\rangle$ are the final and initial states, $\omega_{fi}$ is the transition frequency, $\Gamma$ is the line width and $\omega$ is the frequency of the incident radiation. The incident flux is $\epsilon_0 E^2 c^2/2$ so that the absorption coefficient $K(\omega)$ is given by

$$K(\omega) = N_{3d}\, 4\pi\alpha \frac{\omega_{fi}^2}{\omega} |\langle f|z|i\rangle|^2 \frac{\Gamma}{\Gamma^2 + (\omega_{fi}-\omega)^2} \qquad \text{(A1.7)}$$

where $\alpha = e^2/4\pi\hbar c$

The total absorption integrated through the line is given by

$$N_{3d}\, 4\pi^2\alpha\, \omega_{fi} |\langle f|z|i\rangle|^2 \qquad \text{(A1.8)}$$

We will model the transition by a Lorentzian oscillator by writing

$$\epsilon_2 = \epsilon_\infty + \frac{\Omega_p^2 f_{if}}{\omega^2 - \omega_{fi}^2 - i\gamma\omega} = \epsilon_1(\omega) + i\epsilon_2(\omega) \qquad \text{(A1.9)}$$

$$= \epsilon_\infty + \frac{\Omega_p^2 f_{if}(\omega^2-\omega_{fi}^2)}{(\omega^2-\omega_{fi}^2)+\gamma^2\omega^2} + i\frac{\Omega_p^2 f_{if}\gamma^2\omega^2}{(\omega^2-\omega_{fi}^2)^2+\gamma^2\omega^2}$$

where $\Omega_p^2 = \frac{N_{3D} e^2}{\epsilon_0 m^*}$

The absorption coefficient is given approximately by the expression

$$K(\omega) = \frac{\omega \varepsilon_2(\omega)}{c} \qquad \text{(A1.10)}$$

and the total integrated absorption is

$$\frac{1}{c} \int_0^\infty \omega \varepsilon_2(\omega) d\omega = \frac{\pi}{2c} \omega_p^2 f_{if} \qquad \text{(A1.11)}$$

Equating (A1.11) with (A1.8) so that the total absorption is conserved, we see that

$$f_{if} = \frac{2m^*}{\hbar} \omega_{fi} |\langle f|z|i\rangle|^2 \qquad \text{(A1.12)}$$

Comparing the peak values of the absorption coefficients gives the relation

$$\gamma = \frac{\Gamma}{2}$$

$f_{if}$ is known as the oscillator strength and obeys the well known sum rule

$$\sum_{\text{final states}} f_{if} = 1 \qquad \text{(A1.13)}$$

We now have a model for the dielectric response of the quantum well to electric fields perpendicular to the plane of the well. We will assume that the electrons behave like a free electron gas when subject to an external electric field in the plane of the well and write

$$\epsilon_x = \epsilon_\infty - \frac{\Omega_p^2}{\omega(\omega + i/\tau)} \qquad \text{(A1.14)}$$

This model is essentially the same as that used by Goosen and Lyon[6].

The rate of energy absorption in the quantum well is

$$\frac{|E_{int_z}|^2}{2} \mathrm{Im}\left(\varepsilon(\omega)\right) \qquad \text{(A1.15)}$$

where $E_{int_z}$ is the local transverse electric field in the well and is related to the external field by

$$E_{int_2} = \frac{E_{ext_2}}{\epsilon(\omega)} \qquad \text{(A1.16)}$$

so that (A1.15) becomes

$$\frac{1}{2} \frac{|E_{ext_2}|^2}{|\epsilon(\omega)|^2} \mathrm{Im}\left(\epsilon(\omega)\right) \qquad \text{(A1.17)}$$

Maximum absorption occurs at $\omega^2 = \omega_0^2 + \omega_p^2$ provided that the linewidth is small compared to the frequency of the transition. $\left(\omega_p^2 = \Omega_p^2 / \epsilon_\infty\right)$

APPENDIX 2: MULTILAYER ANISOTROPIC MEDIA

We have a model of the quantum well as a slab of anisotropic dielectric material. In order to calculate observable properties of a real system we need to be able to embed the quantum well(s) into an isotropic medium (e. g. the well cladding). This section describes a matrix method for calculating the optical properties of a multilayer system whose components are anisotropic.

We will first establish some general results on the propagation of electromagnetic radiation in anisotropic media. We will restrict our consideration to uniaxial media whose dielectric tensor can be written in the form

$$\underline{\underline{\varepsilon}} = \begin{pmatrix} \varepsilon_x & \cdot & \cdot \\ \cdot & \varepsilon_x & \cdot \\ \cdot & \cdot & \varepsilon_z \end{pmatrix} \qquad \text{(A2.1)}$$

The electric displacement vector $\underline{D}$ is given by

$$\underline{D} = \varepsilon_0 \, \underline{\underline{\varepsilon}} . \underline{E} \qquad \text{(A2.2)}$$

Maxwells equations for the system are

$$\text{div}\, \underline{D} = 0 \qquad \text{(A2.3)}$$

$$\text{div}\, \underline{B} = 0 \qquad \text{(A2.4)}$$

$$\text{curl}\, \underline{H} = \frac{\partial \underline{D}}{\partial t} \qquad \text{(A2.5)}$$

$$\text{curl}\, \underline{B} = -\frac{\partial \underline{B}}{\partial t} \qquad \text{(A2.6)}$$

The medium is non magnetic so that

$$\underline{B} = \mu_0 \underline{H} \qquad \text{(A2.7)}$$

We will now consider plane waves with $\underline{H}=(0,H_y,0)$ and $\underline{E}$ in the xz plane. All

components vary in space and time as $\exp(-i(\omega t - k_x x - k_z z))$. Using (A2.1) and (A2.2) equations (A2.3) to (A2.6) become

$$k_x \varepsilon_x E_x + k_z \varepsilon_z E_z = 0 \qquad \text{(A2.8)}$$

$$k_z H_y = \varepsilon_0 \varepsilon_x \omega E_x \qquad \text{(A2.9)}$$

$$k_x H_y = -\varepsilon_0 \varepsilon_z \omega E_z \qquad \text{(A2.10)}$$

$$k_z E_x - k_x E_z = \mu_0 \omega H_y \qquad \text{(A2.11)}$$

Eliminating $E_x$, $E_z$ and $H_y$ from (A2.8) to (A2.11) gives the dispersion relation

$$\frac{\omega^2}{c^2} = \frac{k_x^2}{\varepsilon_z} + \frac{k_z^2}{\varepsilon_x} \qquad \text{(A2.12)}$$

(A2.9) and (A2.10) are conveniently re-written in the form

$$E_x = \frac{k_z}{\varepsilon_0 \varepsilon_x \omega} H_y \qquad \text{(A2.13)}$$

$$E_z = \frac{-k_x}{\varepsilon_0 \varepsilon_z \omega} H_y \qquad \text{(A2.14)}$$

Note that (A2.3) implies that $\underline{k}.\underline{D}=0$ so that $\underline{D}$ is perpendicular to $\underline{k}$. $\underline{E}$ will not be perpendicular to $\underline{k}$ so that the Poynting vector $\underline{S}=\underline{E}\times\underline{H}$ is not parallel to $\underline{k}$. The direction of energy propagation is not the same as the direction of the wavevector.

The multilayer systems we are interested in will be stratified in the z direction and the components will be taken to be isotropic in the x y plane. We will only consider TM waves with $\underline{H}$ parallel to y and $\underline{E}$ in the xz plane. (TE waves with $\underline{E}$ parallel to y are not affected by the anisotropy.)

The boundary conditions for wave propagation are:

(i) $k_x$ is constant throughout the system and is set by the angle of incidence and the properties of the initial layer. $k_z$ can then be calculated for each layer using the

dispersion relation (A2.1 ).

(ii) $E_x$ and $H_y$ are continuous at the interfaces.

We will follow the components of $H_y$ associated with forward and backward going waves through each layer. (A forward going wave varies as $\exp(-i(\omega t-k_z z))$ and a backward going wave as $\exp(i(\omega t+k_z z))$.)

Consider first an interface with forward and backward wave amplitudes (components of $H_y$) $(U_2,D_2)$ and $(U_1,D_1)$ to its left and right respectively.

Continuity of $H_y$ gives

$$U_1 + D_1 = U_2 + D_2 \tag{A2.15}$$

and continuity of $E_x$

$$\frac{k_{z_2} U_2}{\epsilon_{x_2}} - \frac{k_{z_2} D_2}{\epsilon_{x_2}} = \frac{k_{z_1} U_1}{\epsilon_{x_1}} - \frac{k_{z_1} D_1}{\epsilon_{x_1}} \tag{A2.16}$$

so that

$$\begin{pmatrix} U_2 \\ D_2 \end{pmatrix} = \begin{pmatrix} \frac{1}{2}\left(1 + \frac{k_{z_1}\epsilon_{x_2}}{k_{z_2}\epsilon_{x_1}}\right) & \frac{1}{2}\left(1 - \frac{k_{z_1}\epsilon_{x_2}}{k_{z_2}\epsilon_{x_1}}\right) \\ \frac{1}{2}\left(1 - \frac{k_{z_1}\epsilon_{x_2}}{k_{z_2}\epsilon_{x_1}}\right) & \frac{1}{2}\left(1 + \frac{k_{z_1}\epsilon_{x_2}}{k_{z_2}\epsilon_{x_1}}\right) \end{pmatrix} \begin{pmatrix} U_1 \\ D_1 \end{pmatrix} \tag{A2.17}$$

$$= (IFM) \begin{pmatrix} U_1 \\ D_1 \end{pmatrix}$$

Similarly U and D at different places within a layer are related by the matrix equation

$$\begin{pmatrix} U(z_2) \\ D(z_2) \end{pmatrix} = \begin{pmatrix} e^{-ik_z\Delta z} & 0 \\ 0 & e^{ik_z\Delta z} \end{pmatrix} \begin{pmatrix} U(z_1) \\ D(z_1) \end{pmatrix} = (PM) \begin{pmatrix} U(z_1) \\ D(z_1) \end{pmatrix} \tag{A2.18}$$

Thus by setting (U,D)= (1,0) at the end of the multilayer, where there can only be an output (forward going) wave and multplying by the appropriate matrices we can obtain the appropriate input wave. (See figure 9.) Allowing $k_z$, $\epsilon_x$ and $\epsilon_z$ to be complex allows surface plasmons, evanescent waves etc. to be handled automatically. Finally we note that

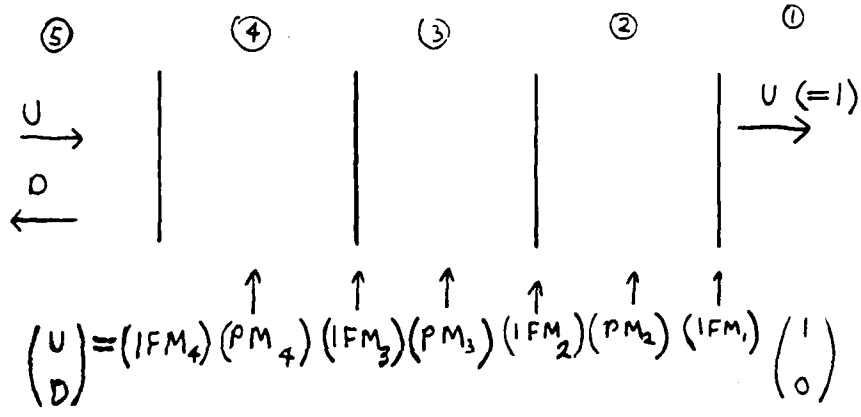


**Figure 9** The structure of the matrix multiplication necessary to calculate the optical properties of a multilayer system.

when the components of $H_y$ are known equations (A2.13) and (A2.14) allow the electric field to be calculated. Once the input and output wave are known it is a simple matter to calculate transmission, absorption and reflection coefficients for the system.

REFERENCES


1 L C West and S J Eglash Appl. Phys. Lett. 46 1156 (1985)

2 A Harwit and J S Harris Jr. Appl. Phys. Lett. 50 685 (1987)

3 B F Levine, R J Malik, J Walker, K K Choi, C G Bethea, D A Kleinman and J M Vandenberg Appl. Phys. Lett. 50 273 (1987)

4 B F Levine, K K Choi, C G Bethea, J Walker, and R J Malik, Appl. Phys. Lett. 50 1092 (1987)

5 D D Coon and R P G Karunasiri Appl. Phys. Lett. 45 649 (1984)

6 M Yu Martisov and A Ya Shik Sov. Phys. Semicond. 20 976 (1986)

7 K W Goosen and S A Lyon Appl. Phys. Lett. 47 1257 (1985)

DOCUMENT CONTROL SHEET

Overall security classification of sheet .....UNCLASSIFIED.....

(As far as possible this sheet should contain only unclassified information. If it is necessary to enter classified information, the box concerned must be marked to indicate the classification eg (R) (C) or (S) )

| 1. DRIC Reference (if known) | 2. Originator's Reference | 3. Agency Reference | 4. Report Security Classification |
|---|---|---|---|
| | MEMO 4018 | | U/C |

| 5. Originator's Code (if known) | 6. Originator (Corporate Author) Name and Location |
|---|---|
| 778 400 | RSRE, St Andrews Road, Malvern, Worcs. WR14 3PS |

| 5a. Sponsoring Agency's Code (if known) | 6a. Sponsoring Agency (Contract Authority) Name and Location |
|---|---|
| | |

7. Title
INFRARED DEVICES USING SEMICONDUCTOR QUANTUM WELLS

7a. Title in Foreign Language (in the case of translations)

7b. Presented at (for conference papers) Title, place and date of conference

| 8. Author 1 Surname, initials | 9(a) Author 2 | 9(b) Authors 3,4 | 10. Date | cc ref |
|---|---|---|---|---|
| KANE, M J | APSLEY, N. | | 1987.11 | 30 |

| 11. Contract Number | 12. Period | 13. Project | 14. Other Reference |
|---|---|---|---|
| | | | |

15. Distribution statement

Descriptors (or keywords)

continue on separate piece of paper

Abstract We describe in this memo the results of a preliminary calculation which shows how the inter subband optical transition in III V quantum wells may be used as the basis for research into a family of infrared devices. In particular, we show that resonating the transition with a surface plasmon or with a guided mode in a semiconductor quantum well metal structure can enhance its optical effects by roughly a factor of 50. This allows only $4 \times 10^{12}$ carriers per sq.cm to effect total absorption of the incoming radiation. Such a density can be controlled electrostatically and so the transition may be switched by applying a bias to the Shottky metal, thus we have an efficient electronic modulator for the 10 micron band. Intersubband absorption should, in addition, show significant photoconductivity and so the device might prove a reasonable infrared detector. Finally an important consideration of this device is that it is built epitaxially using wide band gap semiconductors. The possibilities, therefore, of substantial monolithic integration are considerable and we allow ourselves some speculation on the types of device which may be possible.

SD0/48

END

DATE

FILMED

8